View metadata, citation and similar papers at core.ac.uk
brought to you by CORE
provided by Ghent University Academic Bibliography

INFLUENCE OF CHLORIDE-INDUCED CORROSION ON TENSILE MEMBRANE BEHAVIOUR OF REINFORCED CONCRETE SLABS

Wouter Botte, Robby Caspeele and Luc Taerwe

Magnel Laboratory for Concrete Research, Department of Structural Engineering, Ghent University, Ghent, Belgium

Abstract

Deterioration due to corrosion has been a growing concern in the last decades since it results in a reduction of the cross-section of the reinforcement, cracking and possible loss of the concrete section. Apart from deterioration, also the awareness of the importance of structural robustness has increased due to several failures with progressive collapse. Due to the activation of tensile membrane action in reinforced concrete slabs at large deformations, an alternate load path can be developed which can significantly increase the structural robustness. In this contribution, a validated numerical model for the tensile membrane behaviour of reinforced concrete slabs is used to investigate the influence of corrosion effects on this membrane behaviour. A two-step analysis is adopted: first a cross-section analysis is performed, followed by an analysis of the structural member.

Keywords: Corrosion, Membrane action, RC slabs, FEM analysis, robustness

1 Introduction

In the last decades, deterioration of existing structures has been a growing concern. Deterioration due to corrosion of reinforcement steel has been of particular interest since the associated reduction of the steel section results in a decrease of the structural safety. Another topic which has been the subject of many publications is the assessment of structural robustness. One way to increase structural robustness is to provide an alternate load path. Such an alternate load path can be provided by membrane action.

Both topics, i.e. robustness and deterioration, are combined in this contribution: the influence of chloride-induced corrosion on the membrane behaviour of a reinforced concrete slab is investigated.

In the following sections, a brief introduction to membrane action and the effects of corrosion on reinforcement properties is given. Subsequently, a framework for the FEM analysis of reinforced concrete elements subjected to corrosion is described. Finally, this framework is illustrated through an example reinforced concrete slab subjected to large deformations.

The results of this research are of particular importance in the development of a framework for the assessment of structural robustness of deteriorated concrete structures.

2 Membrane action

Reinforced concrete slabs are generally designed to resist bending moments. The design is traditionally based on small deformation theories. However, in case of an accidental situation, e.g. excessive loading or removal of a support, large deformations are to be expected. At large deformations, the bending behaviour in RC slabs is shifted towards membrane behaviour. This

results in the development of an alternate load path, allowing for additional load transfer towards the (remaining) supports, which can significantly increase the load-bearing capacity of a horizontally restrained slab.

Fig. 1 shows a typical load–displacement diagram for a horizontally unrestrained one-way slab as well as for a fully restrained slab.

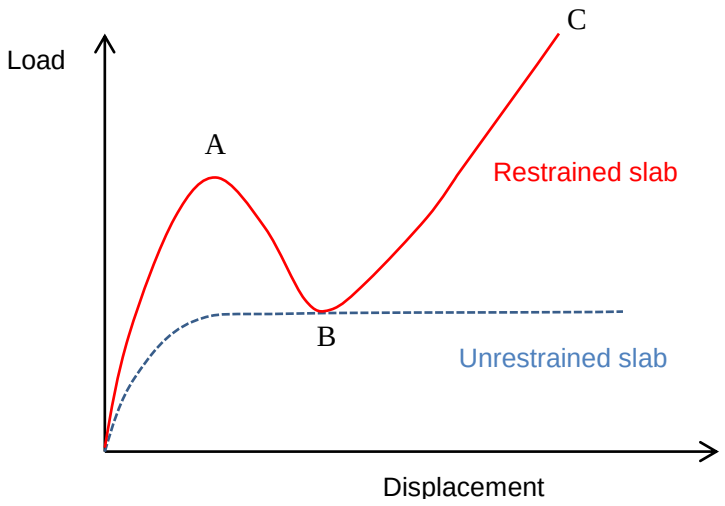

Fig. 1 Load-displacement behaviour of restrained and unrestrained RC slabs

In case no horizontal restraint is present, the one-way slab will deflect under the applied load until a yielding plateau establishes and the slab fails either due to concrete crushing or rupture of the reinforcement. No increase in the load-carrying capacity is observed.

Considering a slab with perfect edge restraints against lateral displacement, compressive membrane action is induced at small deflections due to the restrained outward movement along the slab edges. This may offer a much higher flexural load than the maximum load predicted by Johansen's Yield Line Theory (1962), especially in case of elements with small slenderness. After the outermost flexural load has been reached in point A, the load-displacement graph shows a rapid decrease of the supported load with further increasing deflection as a result of the reduction of compressive membrane forces. Further, near point B, membrane forces reach the stage where they change from compression to tension. The slab's boundary restraints start to resist inward movement of the edges. Accordingly, cracks extend over the full thickness of the slab and the yielding of steel reinforcement is established due to the elongation of the slab surface. It is observed that beyond point B the reinforcement acts as a tensile net that enables additional load-carrying capacity under increasing deflections. The load increases for a second time until the rupture of the reinforcement at point C. It is obvious that in this case, reinforcement properties have a big influence on the ultimate bearing capacity of the slab.

In case of robustness quantification, the quantification of the residual capacity of the alternative load path established by the development of tensile membrane action becomes of crucial importance.

3 Corrosion

A common deterioration mechanism in reinforced concrete is corrosion of the reinforcement steel. Corrosion affects the steel as well as the concrete by (Rodriguez et al. 1997):

- Reduction of the bar section;
- Reduction of the mechanical properties of the steel;
- Cracking and spalling of the concrete due to the expansion of corrosion products;

- Bond deterioration between the steel and the surrounding concrete.

Because of these phenomena, the safety of deteriorated concrete structures is reduced. According to the Model Code for Service Life Design (*fib* 2006), the process of corrosion of the reinforcement can be divided roughly into two time periods: the initiation period and the propagation period. The first phase is defined as the time until the reinforcement becomes depassivated, either by chloride ingress or by carbonatation. During the second phase, the reinforcement itself is affected: the net cross-section is reduced and corrosion products accumulate, resulting in a volumetric expansion of the bars. Both the initiation and propagation phase are governed by different stochastic parameters and can be described by mathematical models. In this contribution, only the propagation phase will be considered.

3.1 Influence on the cross-section

Once corrosion is initiated, the corrosion rate is determined by equation (1), as proposed by Vu & Stewart (2000) and Stewart & Suo (2009):

$$i_{corr}(t_p) = i_{corr}(0) \cdot 0.85 t_p^{-0.29} \tag{1}$$

where $i_{corr}(t_p)$ [μA/cm²] is the corrosion rate at time t_p, t_p [years] is the time since corrosion initiation and $i_{corr}(0)$ [μA/cm²] is the corrosion rate at the start of corrosion propagation. The latter can be calculated from:

$$i_{corr}(0) = \frac{2.70\,(1-w/c)^{-1.64}}{a} \tag{2}$$

where w/c [-] is the water cement ratio and a [cm] is the concrete cover. It follows from equation (1) that the corrosion rate decreases in time, which is due to the formation of rust products on the steel surface, obstructing the diffusion of the iron ions away from the steel surface (Vu & Stewart 2000).

Equation (1) is only valid when no spalling occurs. In case spalling does occur, the corrosion rate can be assumed to be constant i_{corr} = 0.0119 μA/cm² (Papadopoulos et al. 2011).

As suggested by Stewart & Rosowsky (1998), the reduction in bar radius of the reinforcement steel can be derived from the corrosion rate (since 1 μA/cm² = 0.0116 mm/year):

$$X(t_p) = 0.0116 \int_0^{t_p} i_{corr}(t)dt \tag{3}$$

where $X(t_p)$ [mm] is the corrosion attack depth t_p years after corrosion initiation (Fig. 2).

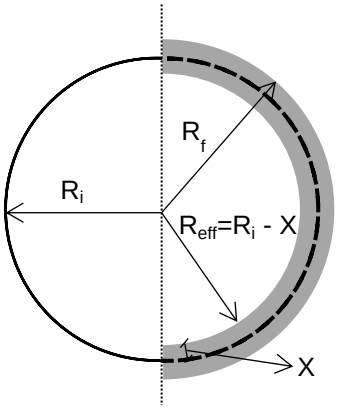

Fig. 2 Dimensions of the reinforcement cross-section, before and after corrosion

According to Molina et al. (1993) and Coronelli & Gambarova (2004), the ratio of the specific volumes of the corrosion products with respect to steel is equal to 2, therefore the diameter of the reinforcement bar increases by 2X.

3.2 Influence on the stress-strain diagram

Several authors (W.W. Aldridge et al. 1970, T. Uomoto and S. Misra 1984, M. Maslehuddin et al. 1990, A.A. Almusallam 2001) indicated that the effect of corrosion on the yield strength and ultimate strength is marginal when the stress is calculated using the actual (reduced) area of the cross-section, hence such a reduction is not considered in this contribution. However, it was reported that the ductility of the reinforcing steel decreased significantly due to corrosion. A simplified approach is introduced here in order to describe this phenomenon, since no accurate models for this reduction are found in literature. The reduction of the ultimate reinforcement strain $\varepsilon_{su,red}$ due to corrosion is calculated through the (linear) equation (4) based on research mentioned in (Coronelli & Gambarova 2004) and (Hingorani et al. 2013):

$$\varepsilon_{su,red} = \varepsilon_{sy} + (\varepsilon_{su} - \varepsilon_{sy})\left(1 - \frac{\alpha}{\alpha_{max}}\right) \tag{4}$$

$$\alpha = \frac{\Delta A}{A_0} \tag{5}$$

where ε_{su} is the ultimate strain of the reinforcement without corrosion, ε_{sy} is the strain corresponding to the yield stress, α is the percent of reduction of the bar cross-section, ΔA is the area reduction due to corrosion, A_0 is the nominal area of the reinforcement bar and α_{max} is the maximum reduction of the bar cross-section. Since brittle failure is observed when the cross-section is reduced to 50% of the initial cross-section, α_{max} is assumed to be equal to 0.5 (Palsson and Mirza 2002).

3.3 Influence on the bond strength (Bhargava et al. 2007)

Experimental research shows that the bond strength between concrete and reinforcement is significantly influenced by corrosion. A wide scatter in the magnitudes of the bond strength and the effect of corrosion on it has been observed, since the results are based on a wide variety of specimens and bar types.

In the present study, the empirical model developed by Bhargava et al. (2007) was adopted to describe the bond deterioration due to corrosion. This model is based on a large set of different pull-out tests, as depicted in Fig. 3. The normalized bond strength R is defined as the ratio of the bond strength at a certain corrosion level to the original bond strength for the un-corroded specimen

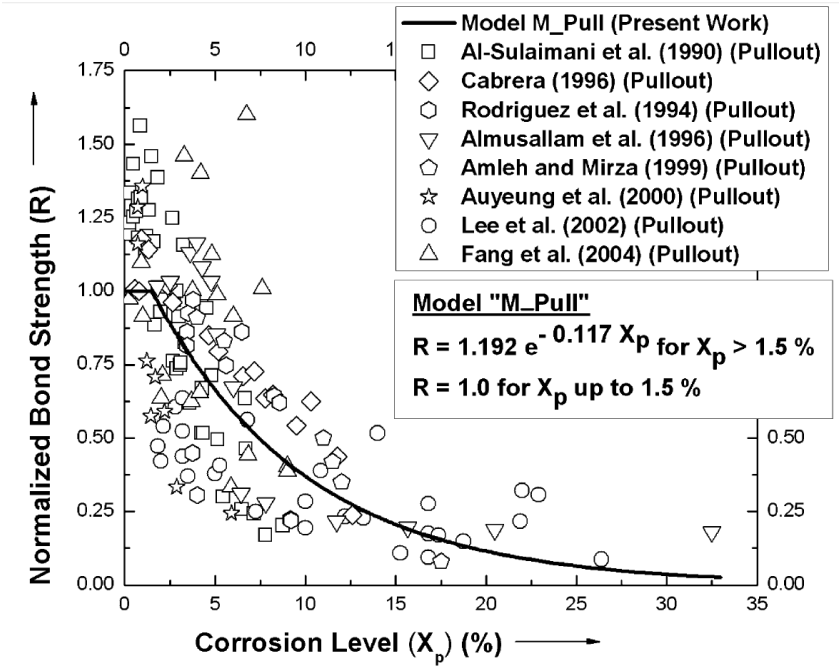

Fig. 3 Normalized bond strength as a function of the corrosion level (Bhargava et al. 2007)

The normalized bond strength is a function of the corrosion level X_p, which is the loss of weight of the reinforcing bar expressed as a percentage of the original rebar weight, according the following equation:

$$R(X_p) = \begin{cases} 1.0 & if\ X_p \leq 1.5\% \\ 1.192e^{-0.117X_p} & if\ X_p > 1.5\% \end{cases} \quad (6)$$

4 FEM methodology (Sánchez et al. 2010)

In order to model the mechanical behaviour of reinforced concrete slabs affected by corrosion, the framework developed by Sánchez et al. (2010) was adopted. This finite element methodology is able to simulate the structural deterioration of corroded reinforced concrete elements. The methodology is capable of reproducing many of the mechanical effects induced by corrosion processes in reinforced concrete elements, e.g. expansion of the reinforcement bars due to the corrosion product accumulation, damage and crack pattern in the surrounding concrete, degradation of steel-concrete bond stress transfer, net area reduction in the reinforcements and the influence of all these mechanisms on the structural load carrying capacity predictions.

Two different (and coupled) mesoscopic analyses are considered in order to describe the aforementioned phenomena: (i) an analysis at the structural member cross-section level; (ii) an analysis at the structural member level. The finite element analyses for this contribution are performed using the TNO Diana software.

4.1 Description of the structural member

The structural member that is considered, is a reinforced concrete slab. The dimensions and material properties of this slab are based on the experimental research performed by Gouverneur et al. (2013). The aim of this research was to investigate the effect of tensile membrane action on the ultimate load-bearing capacity of a reinforced concrete slab. This was done by the artificial removal of an intermediate support of a statically indeterminate concrete slab.

Based on this experimental research, a numerical model was developed, which is capable of predicting the ultimate load-bearing capacity of a slab at large deformations (i.e. under tensile membrane action). This model is now used in the 2D longitudinal analysis.

A general overview of the slab under consideration is given in Fig. 4. It is a 180 mm thick and 1800 mm wide reinforced concrete slab strip, supported at five points and fully restrained in the horizontal direction. The total length is 14.30 m with the distance between the inner supports and the central support being 4 m, changing to one span of 8 m after the removal of the latter, simulating an accidental situation that triggers membrane action. The longitudinal reinforcement is continuous over the entire length and consists of 16 bars with a nominal diameter of 10 mm for both the bottom and top reinforcement layer, with a concrete cover of 20 mm.

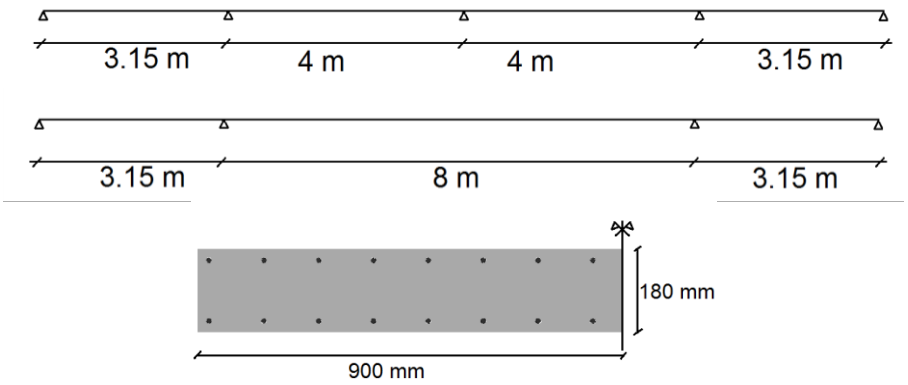

Fig. 4 Dimensions of the slab: (a) longitudinal model before accidental situation; (b) longitudinal model after accidental situation; (c) cross-section.

The material properties before corrosion starts, are listed in Table 1.

Table 1 Material properties

Property	**Value**
Concrete compressive strength f_c	36 MPa
Concrete tensile strength f_{ct}	2.8 MPa
Concrete Young's modulus E_c	30 000 MPa
Top/bottom reinforcement cross-section A_0	1256 mm²
Reinforcement yield stress f_y	555 MPa
Reinforcement Young's modulus E_s	210 000 MPa
Reinforcement tensile strength f_t	605 MPa
Ultimate strain of reinforcement ε_u	8.04 %

In the following sections, it is assumed that the top reinforcement is subjected to corrosion.

4.2 Cross-section analysis

In the first step, the reinforcement expansion due to the volume increase of the steel bars as a consequence of corrosion product accumulation is simulated in a two-dimensional plane strain cross-sectional model. The damage distribution and crack patterns in the concrete are evaluated, which defines the concrete net section loss in the structural member.

For this first step, a linear elastic constitutive relation is adopted for the steel rebars. The expansion due to the corrosion products is simulated by a volumetric deformation of the steel rebars. The dilatational component D of the total strain can be obtained from the following expression (Sánchez et al. 2010):

$$D \approx \frac{R_f^2(X) - R_i^2}{2R_i^2} \tag{7}$$

where R_i is the initial value of the bar radius (i.e. 5 mm) and $R_f(X)$ is the (corroded) final value of the bar radius, which depends on the corrosion attack depth X (section 3.1). As mentioned in section 3.1, the value R_f can considered to be $R_f = R_i + X$, which is based on the assumption that the corrosion products are incompressible.

The concrete compressive behaviour is implemented as a bi-linear stress-strain relationship and the Hordijk tension softening model is adopted for concrete in tension. The stiffness adaptation method is used to calculate the crack pattern and crack-widths. A stiffness adaptation analysis performs a sequence of linear static analysis, where in a subsequent iteration the elastic stiffness is reduced (E_0 to E_1, Fig. 5) in those integration points in which the stresses in a previous iteration were beyond the specified stress-strain curve (σ_0, Fig. 5). After a certain amount of iterations, the stress-strain combinations for all integration points are on this curve. The output of the analysis is, amongst others, the stiffness reduction factor *d*, which is a measure for the extent of the damage to the concrete ($E_1 = d.E_0$). The stiffness adaptation analysis can be used efficiently for calculating crack patterns and crack openings in serviceability loading conditions (Schreppers et al. 2011).

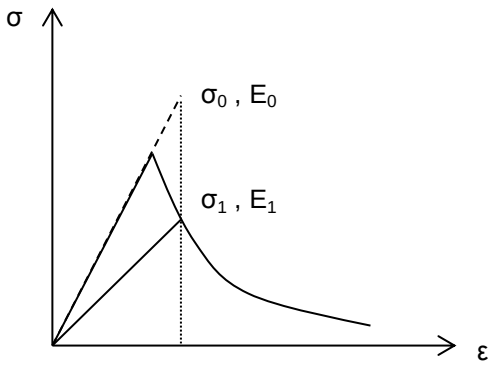

Fig. 5 Stress strain curve with stress and stiffness reduction (Schreppers et al. 2011)

As an example, the output of the cross-section analysis is illustrated in Fig. 6 for a corrosion level of 1%. It can be seen that cracks develop from the reinforcement bars towards the concrete surface, which leads to a stiffness reduction is these areas.

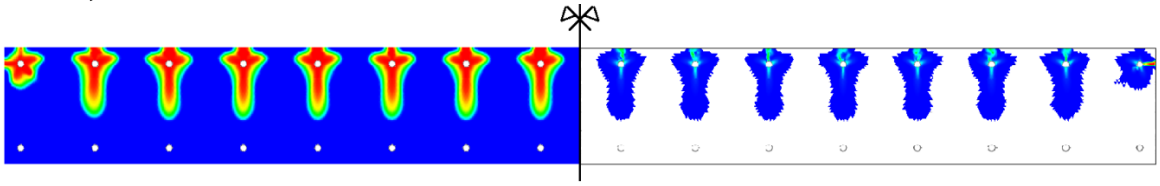

Fig. 6 Stiffness reduction factor (left) and crack pattern (right), for corrosion level = 1%.

4.3 2D longitudinal analysis

Considering the results of the previous analysis, the mechanical response of the structural member subjected to an external load is determined. This results in the global response of the element under consideration, as well as the failure mechanism.

As a result of the symmetry of the specimen regarding its geometry and loading, only half of the specimen is modelled. The geometrical nonlinearity was taken into account by a total Lagrange approach. For reinforcement, one-dimensional fully embedded bar reinforcement (truss elements) is applied. For the longitudinal analysis, a multi-linear stress-strain relationship is applied for the reinforcement steel. Note that also the sudden decrease in strength after rupture of the reinforcement bars was considered as it was the intention to investigate the slabs up to failure. Further, the strain hardening hypothesis together with the Von Mises plastic criterion is used. Finally, a full nonlinear analysis is required, in order to accurately simulate the tensile membrane

behaviour in the slab. This tensile membrane behaviour develops after the removal of the middle support.

4.4 Coupling between cross-sectional analysis and 2D longitudinal analysis

The cross-sectional analysis is performed until a certain corrosion depth X (section 3.1 and 4.2). For this corrosion depth, the results of the cross-section analysis are investigated. If there are cracks crossing the concrete cover, then the part of the section that is located on the outside is removed, i.e. provides no stiffness (d = 0).

Subsequently, the cross-section is divided into horizontal slices and the average value for the damage *d* is determined for each slice. This is projected on to the 2D longitudinal model. Further, for each corrosion depth X, the reduction of the reinforcement steel properties are determined (i.e. the reduction of the cross-section, ultimate reinforcement strain and bond strength). These steps result in an updated model and finally the longitudinal analysis is performed. Failure of the slab is observed to be related to the strain of the reinforcement.

5 Results

Fig. 7 shows the load-displacement response (a) and the corresponding membrane forces (b) for the reinforced concrete slab, for different corrosion levels, in case the cross-sectional analysis is not performed. The latter means that only the reduction of the steel properties is taken into account and the cracking (and stiffness reduction) of the concrete is not. The corrosion level α is expressed as the percent of reduction of the bar cross-section, defined by (5) in section 3.2.

The general behaviour is as described in section 2. A first load-peak is observed at a load level of 100 kN. This load-peak is due to compressive membrane action and is almost the same for all corrosion levels, i.e. corrosion has almost no influence on compressive membrane action. The maximum compressive membrane force exceeds 1500 kN, as can be seen on Fig. 7b.

After this first load-peak, the load decreases until 50 kN and increases again, up to failure of the top reinforcement over the intermediate supports. This second increase is related to the development of tensile membrane forces. It is noted that now corrosion does have an influence: an increase in the corrosion level results in a significant decrease of the load-bearing capacity, even at low corrosion levels (Fig. 7c): the ultimate load is reduced from 236 kN (α = 0%) to 213 kN, 193 kN, 165 kN, 155 kN and 120 kN at corrosion levels of 1%, 2%, 5%, 7.5% and 10% respectively. This reduction of the load-bearing capacity can be attributed to the decrease of the reinforcement properties: the lower ultimate tensile capacity due to the reduced cross-section and the reduced ductility due to the decrease of the ultimate reinforcement strain.

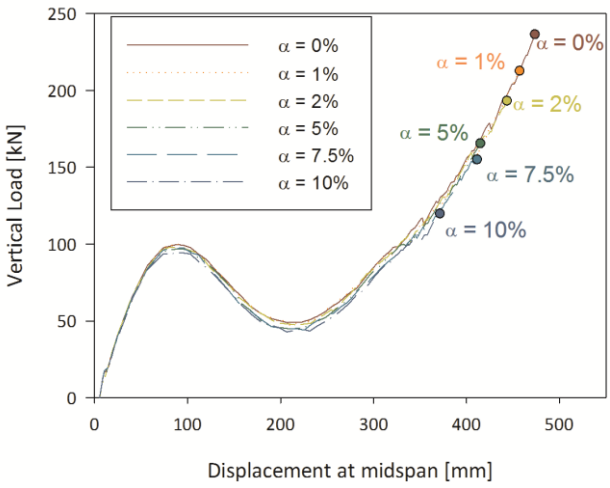

(a)

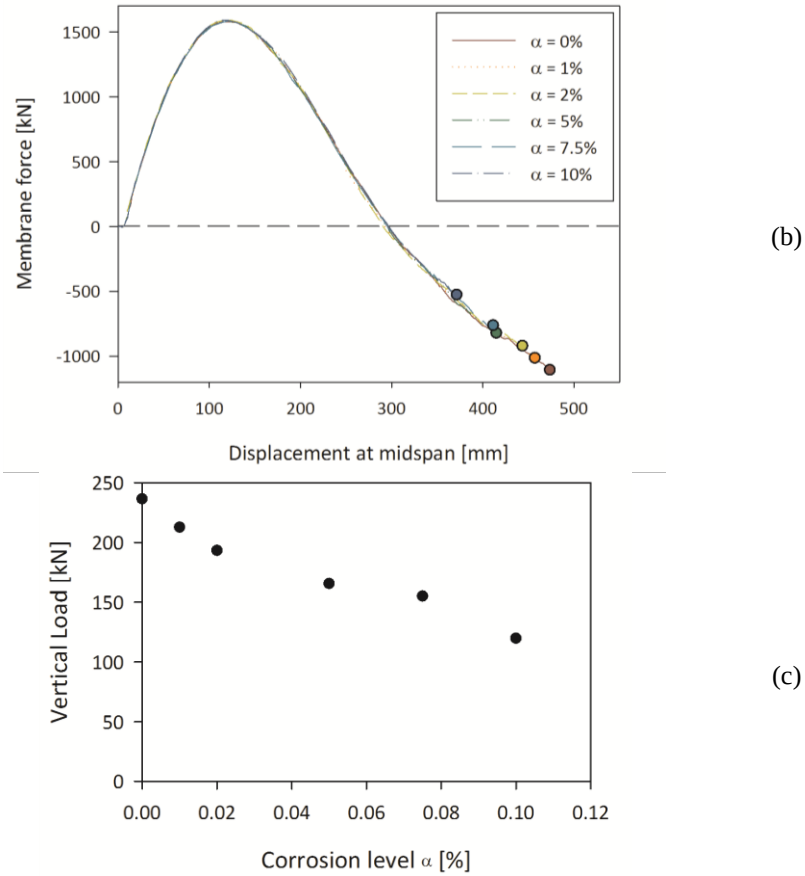

Fig. 7 Load-displacement response (a); membrane forces (b) in the slab and load-bearing capacity as a function of the corrosion level α (c) without considering cracking and stiffness reduction.

Similar calculations have been performed, now taking into account the degradation of the concrete layers due to expansion of the reinforcement bars. The results are represented in Fig. 8. Taking the cracking and reduced stiffness into account results in a less stiff load-displacement response in case of small displacements. Moreover, the load-peak due to compressive membrane action is significantly reduced. However, it is noted that no significant difference between the ultimate load-carrying capacity is obtained in case the cross-sectional analysis is taken into account and the one obtained without this analysis. Indeed, since failure of the concrete slab occurs in the tensile membrane region, the ultimate load is mainly governed by the reinforcement properties and less by the properties of the concrete.

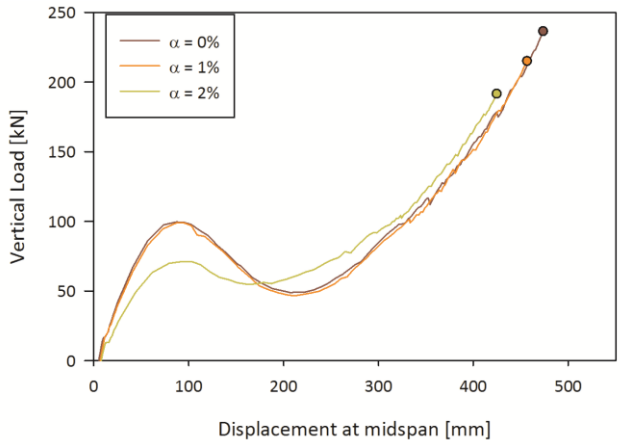

Fig. 8 Load-displacement response taking into account cross-sectional analysis

It is important to note that the results obtained in this contribution are calculated by using a simplified approach to determine the reduction of the ultimate strain of the reinforcement due to corrosion. Moreover it was assumed that the corrosion process was uniform in all cross-sections. Hence, the obtained results should be treated with care, since localized corrosion effects can occur. If these effects are not taken into account, the predictions based on the previous methodology are non-conservative. In those cases, the model should be expanded by using models which explicitly take into account the spatial distribution.

6 Conclusion

In this contribution, a two-step finite element analysis was used to predict the ultimate load-bearing capacity of a reinforced concrete slab subjected to uniform corrosion. During the first step of the analysis, the volumetric expansion of the reinforcement was simulated in a cross-sectional model of the slab. The results of this analysis, i.e. the stiffness reduction due to cracking of the concrete, was subsequently projected on a longitudinal model of the slab. Taking into account the reduced properties of the reinforcement, this model allowed to calculate the ultimate load-bearing capacity of the reinforced concrete slab for different corrosion levels. It was observed that even for small corrosion levels, there was a significant decrease of the ultimate bearing capacity of the slab. This decrease was mainly attributed to the reduced properties of the reinforcement, since there was no difference found between the ultimate load obtained through the two-step analysis and the one obtained through the analysis where only the reduction of the reinforcement properties was considered. The reduction of the properties of the concrete had only an influence on the load-peak caused by compressive membrane action. This compressive membrane stage was however not determining for failure of the slab under consideration in this contribution.

Acknowledgements

Wouter Botte is a Research Assistant of the FWO Research Foundation Flanders. The authors wish to thank the FWO for the financial support on the research project “Structural reliability and robustness assessment of existing structures considering membrane action effects and Bayesian updating of test information”.

References

Aldridge, W.W., Jaffarazadeh, M., Farhadi, K. (1970) Effect of corrosion and bar spacing on bond properties of reinforcing bar in concrete, University of Oklahoma Research Institute

Almusallam, A.A. (2001) Effect of degree of corrosion on the properties of reinforcing steel bars. Construction and Building Materials 15, 361-368

Bhargava, K., Ghosh, A.K., Mori, Y., Ramanujam, S. (2007) Corrosion-induced bond strength degradation in reinforced concrete – analytical and empirical models. Nuclear Engineering and Design 237, 1140–1157

Coronelli, D. & G., Gambarova, P. (2004) Structural assessment of corroded reinforced concrete beams: modeling guidelines. J. Struct. Eng. ASCE 130(8), 1214-1224

Fib Bulletin 34 (2006) Model Code for Service Life Design, Féd. Int. du Béton (fib), Lausanne, Switzerland

Gouverneur, D., Caspeele, R. & Taerwe, L. 2013. Experimental investigation of the load-displacement behaviour under catenary action in a restrained reinforced concrete slab strip. Engineering Structures 49: 1007-1016.

Hingorani, R., Pérez, F., Sánchez, J., Fullea, J., Andrade, C., Tanner, P. (2013) Loss of ductility and strength of reinforcing steel due to pitting corrosion, VIII International conference on fracture mechanics of concrete and concrete structures

Johansen, K.W. (1962) Yield-Line Theory. London: Cement and Concrete Association.

Maslehuddin, M., Ibrahim, I.M., Al-Sulaimani, G.J., Al-Mana, A.I., Abduljauwad, S.N. (1990) Effect of rusting of reinforcing steel on its mechanical properties and bond with concrete. ACI Mater J, 496-502

Molina, F.J., Alonso, C., Andrade, C. (1993) Cover cracking as a function of rebar corrosion. II: numercial model. Materials and Structures 26, 532-548

Palsson, R. & Mirza, M.S. (2002) Mechanical response of corroded steel reinforcement of abandoned concrete bridge. ACI Struct. J. 99(2), 157-162

Papadopoulos, M. P., Apostolopoulos, C. A., Zervaki, A. D. & Haidemenopoulos, G. N. (2011) Corrosion of exposed rebars, associated mechanical degradation and correlation with accelerated corrosion tests. Construction and Building Materials, 25, 3367-3374.

Rodriguez, J., Ortega, L. M. & Casal, J. (1997) Load carrying capacity of concrete structures with corroded reinforcement. Construction and Building Materials, 11, 239-248.

Sánchez, P.J., Huespe, A.E., Oliver, J., Toro, S. (2010), Mesoscopic model to simulate the mechanical behavior of reinforced concrete members affected by corrosion. International Journal of Solids and Structures 47, 559-570

Schreppers, G.J., Frissen, C., Kang, H.J. (2011) Prediction of crack-width and crack-pattern, TNO DIANA

Stewart, M. G. & Rosowsky, D. V. (1998) Time-dependent reliability of deteriorating reinforced concrete bridge decks. Structural Safety, 20, 91-109.

Stewart, M. G. & Suo, Q. (2009) Extent of spatially variable corrosion damage as an indicator of strength and time-dependent reliability of RC beams. Engineering Structures, 31, 198-207.

Uomoto, T., Misra, S. (1984), Behaviour of concrete beams and columns in marine environment when corrosion of reinforcing bars takes place. Detriot: ACI Spec. Publ. SP-109, American Concrete Institute, 127-146.

Vu, K. A. T. & Stewart, M. G. (2000) Structural reliability of concrete bridges including improved chloride-induced corrosion models. Structural safety, 22, 313-333.